Pore Size Control of Highly Ordered Mesoporous Silica MCM-48

Markus Widenmeyer and Reiner Anwander*

Anorganisch-chemisches Institut, Technische Universität München, Lichtenbergstrasse 4, D-85747 Garching, Germany

Received November 9, 2001. Revised Manuscript Received January 30, 2002

The synthesis of highly ordered cubic mesoporous silica MCM-48 with tunable pore sizes in the range 1.6−3.8 nm is reported. Pore size control has been achieved by using (mixtures of) *gemini* surfactants, $[CH_3(CH_2)_nNMe_2(CH_2)_mNMe_2(CH_2)_nCH_3]^{2+}2Br^-$, of different average chain length ($m = 12$ and $n = 15$, 21) as a structure-directing agent and by hydrothermal restructuring at pH > 9 and temperatures >100 °C. A *mesoporosity index*, *M*, is introduced to describe porosity features of periodic mesoporous silica (PMS) materials. *M* is shown to provide distinct values for high quality MCM-48 (*M* 0.34−0.35) and MCM-41 materials (*M* 0.29−0.31) and to sensitively indicate microporosity in mesoporous and macroporous solids. Surface silylation based on tetramethyldisilazane, $HN(SiHMe_2)_2$, reveals different surface silanol populations in dependency of the pore size, and hence, of the surface curvature.

Introduction

The chemistry of advanced materials is getting increasingly attracted by the family of periodic mesoporous silica materials, PMSs.[1] Topological design of PMSs, that is, control of pore architecture and pore size, displays the ultimate approach to tailor their properties for catalytic, adsorptive, and semiconducting applications.[2] Pore size engineering of MCM-41, the original 2-D hexagonal PMS, and in particular pore enlargement has been achieved by various synthetic strategies using, for example, additives such as 1,3,5-substituted benzenes,[1,3] *long-chain* alkyls,[4] *long-chain* alkylamines,[5] or *long-chain* surfactants,[6] and mixed surfactants.[7] Additionally, hydrothermal restructuring procedures were applicable for the synthesis of pore-enlarged MCM-41.[7−9] The discovery of silica SBA-15 seemed to unlimit pore size control of 2-D hexagonal silica phases in the meso regime.[10] However, the synthesis of MCM-48, a 3-D cubic PMS, with adjustable pore sizes appeared to be less straightforward. There are only a few reports dealing with silica MCM-48 featuring pore diameters larger than 3 nm according to the BJH method.[11,12] Cationic *gemini* surfactants of type $[CH_3(CH_2)_nNMe_2(CH_2)_mNMe_2(CH_2)_nCH_3]^{2+}2Br^-$ ($m = 12$) were employed to selectively produce the MCM-48 phase.[13−16] For $n = 17$ and by applying two sequential postsynthetic hydro-

* Corresponding author. Fax: +49 89 289 13473. E-mail: reiner.anwander@ch.tum.de.

(1) (a) Kresge, C. T.; Leonowicz, M. E.; Roth, W. J.; Vartuli, J. C.; Beck, J. S. *Nature (London)* **1992**, *359*, 710. (b) Beck, J. S.; Vartuli, J. C.; Roth, W. J.; Leonowicz, M. E.; Kresge, C. T.; Schmitt, K. D.; Chu, C. T.-W.; Olson, D. H.; Sheppard, E. W.; McCullen, S. B.; Higgins, J. B.; Schlenker, J. L. *J. Am. Chem. Soc.* **1992**, *114*, 10834.

(2) (a) Schüth, F. *Ber. Bunsen-Ges. Phys. Chem.* **1995**, *99*, 1306. (b) Sayari, A. *Stud. Surf. Sci. Catal.* **1996**, *102*, 1. (c) Zhao, X. S.; Lu, G. Q.; Millar, G. J. *Ind. Eng. Chem. Res.* **1996**, *35*, 2075. (d) Corma, A. *Chem. Rev.* **1997**, *97*, 2373. (e) Biz, S.; Occelli, M. L. *Catal. Rev.−Sci. Eng.* **1998**, *40*, 329. (f) Corma, A.; Kumar, D. *Stud. Surf. Sci. Catal.* **1998**, *117*, 201. (g) Clark, J. H.; Macquarrie, D. J. *Chem. Commun.* **1998**, 853. (h) Moller, K.; Bein, T. *Chem. Mater.* **1998**, *10*, 2950. (i) Ciesla, U.; Schüth, F. *Microporous Mesoporous Mater.* **1999**, *27*, 131. (j) Guizard, C. G.; Julbe, A. C.; Ayral, A. *J. Mater. Chem.* **1999**, *9*, 55. (k) Ying, J. Y.; Mehnert, C. P.; Wong, M. S. *Angew. Chem.* **1999**, *111*, 58; *Angew. Chem., Int Ed.* **1999**, *38*, 56.

(3) (a) Huo, Q.; Margolese, D. I.; Ciesla, U.; Demuth, D. G.; Feng, P.; Gier, T. E.; Sieger, P.; Firouzi, A.; Chmelka, B. F.; Schüth, F.; Stucky, G. D. *Chem. Mater.* **1994**, *6*, 1176. (b) Kimura, T.; Sugahara, Y.; Kuroda, K. *Chem. Commun.* **1998**, 559. (c) Anwander, R.; Nagl, I.; Widenmeyer, M.; Engelhardt, G.; Groeger, O.; Palm, C.; Röser, T. *J. Phys. Chem., B* **2000**, *104*, 3532.

(4) (a) Ulagappan, N.; Rao, C. N. R. *Chem. Commun.* **1996**, 2759. (b) Blin, J. L.; Otjacques, C.; Herrier, G.; Su, B.-L. *Langmuir* **2000**, *16*, 4229. (c) Blin, J. L.; Herrier, G.; Otjacques, C.; Su, B.-L. *Stud. Surf. Sci. Catal.* **2000**, *125*, 57. (d) Blin, J. L.; Herrier, G.; Otjacques, C.; Su, B.-L. *Stud. Surf. Sci. Catal.* **2000**, *125*, 75.

(5) (a) Sayari, A.; Kruk, M.; Jaroniec, M.; Moudrakowski, I. L. *Adv. Mater.* **1998**, *10*, 1376. (b) Sayari, A.; Yang, Y.; Kruk, M.; Jaroniec, M. *J. Phys. Chem., B* **1999**, *103*, 3651. (c) Kruk, M.; Jaroniec, M.; Sayari, A. *J. Phys. Chem., B* **1999**, *103*, 4590. (d) Sayari, A. *Angew. Chem.* **2000**, *112*, 3042; *Angew. Chem., Int Ed.* **2000**, *39*, 2920. (e) Kruk, M.; Jaroniec, M.; Sayari, A. *Microporous Mesoporous Mater.* **2000**, *35*, 545.

(6) Ryoo, R.; Ko, C. H.; Park, I.-S. *Chem. Commun.* **1999**, 1423.

(7) (a) Huo, Q.; Margolese, D. I.; Stucky, G. D. *Chem. Mater.* **1996**, *8*, 1147. (b) Namba, S.; Mochizuki, A.; Kito, M. *Chem. Lett.* **1998**, 569.

(8) (a) Khushalani, D.; Kuperman, A.; Ozin, G. A.; Tanaka, K.; Garces, J.; Olken, M. M.; Coombs, N. *Adv. Mater.* **1995**, *7*, 842. (b) Sayari, A.; Liu, P.; Kruk, M.; Jaroniec, M. *Chem. Mater.* **1997**, *9*, 2499. (c) Kruk, M.; Jaroniec, M.; Sayari, A. *Microporous Mesoporous Mater.* **1999**, *27*, 217.

(9) (a) Corma, A.; Kan, Q.; Navarro, M. T.; Pérez-Pariente, J.; Rey, F. *Chem. Mater.* **1997**, *9*, 2123. (b) Cheng, C.-F.; Zhou, W.; Park, D. H.; Klinowski, J.; Hargreaves, M.; Gladden, L. F. *J. Chem. Soc., Faraday Trans.* **1997**, *93*, 359.

(10) (a) Zhao, D.; Feng, J.; Huo, Q.; Melosh, N.; Friedrickson, G. H.; Chmelka, B. F.; Stucky, G. D. *Science* **1998**, *279*, 548. (b) Zhao, D.; Huo, Q.; Feng, J.; Chmelka, B. F.; Stucky, G. D. *J. Am. Chem. Soc.* **1998**, *120*, 6024.

(11) Corma, A.; Kan, Q.; Rey, F. *Chem. Commun.* **1998**, *579*.

(12) (a) Ryoo, R.; Joo, S. H.; Kim, J. M. *J. Phys. Chem., B* **1999**, *103*, 7435. (b) Kruk, M.; Jaroniec, M.; Ryoo, R.; Joo, S. H. *Chem. Mater.* **2000**, *12*, 1414.

(13) Huo, Q.; Leon, R.; Petroff, P. M.; Stucky, G. D. *Science* **1995**, *268*, 1324.

(14) (a) Van Der Voort, P.; Morey, M.; Stucky, G. D.; Mathieu, M.; Vansant, E. F. *J. Phys. Chem., B* **1998**, *102*, 585. (b) Van Der Voort, P.; Mathieu, M.; Mees, F.; Vansant, E. F. *J. Phys. Chem., B* **1998**, *102*, 8847. (c) Van Der Voort, P.; Baltes, M.; Vansant, E. F. *J. Phys. Chem., B* **1999**, *103*, 10102. (d) Benjelloun, M.; Van Der Voort, P.; Cool, P.; Collart, O.; Vansant, E. F. *Phys. Chem. Chem. Phys.* **2001**, *3*, 127.

(15) Morey, M. S.; Davidson, A.; Stucky, G. D. *J. Porous Mater.* **1998**, *5*, 195.

10.1021/cm011273b CCC: $22.00
Published on Web 03/28/2002

Table 1. Synthetic Details and Important Pore Parameters of MCM-48 Materials under Study

sample	chain length[a]	no. of hydrothermal treatments (T/pH/t)[b]	a[c]/nm	V_p[d]/cm^3 g^{-1}	$d_{p,ads}$[e]/nm (fwhm/nm)	$d_{p,des}$[e]/nm (fwhm/nm)	a_s(BET)[f]/ m^2 g^{-1}	M[g]
1	16	1 (100(8.5/7 d)	6.78	0.80	1.9 (0.5)	1.6 (0.5)	ca. 1450[h]	
2	16	1 (100/8.5/3 w)	7.35	0.92	2.1 (0.5)	1.8 (0.5)	ca. 1500[h]	
3	16	1 (110/8.5/3 w)	7.78	1.05	2.2 (0.5)	2.0 (0.5)	ca. 1550[h]	
4	16	2 (110/8.5/6 w)	8.51	0.97	2.3 (0.3)	2.1 (0.3)	1330	0.35
5	16	2 (100/12.5/5 w)[i]	8.19	0.97	2.3 (0.2)	2.2 (0.2)	1350	0.33
6	16/22	1 (100/8.5/3 w)	9.01	1.18	2.6 (0.4)	2.5 (0.4)	1380	0.34
7	22	1 (100/8.5/3 w)	9.52	1.35	2.9 (0.4)	2.8 (0.4)	1340	0.35
8	22	2 (100/11/7 w)	10.01	1.12	3.2 (0.2)	3.0 (0.2)	1070	0.35
9	22	1 (110/8.5/3 w)		1.33	3.3 (0.3)	3.2 (0.25)	1250	0.34
10	22	2 (110/10/4 w)	10.65	1.21	3.6 (0.2)	3.4 (0.15)	1050	0.34
11	22	3 (120/11.5/6 w)	10.65	1.02	3.7 (0.2)	3.5 (0.2)	950	0.31[j]
12	22	1 (130/8.5/5 d)	12.15	0.74	4.1 (0.4)	3.8 (0.3)	750	0.26[j]
13	22	3 (130/7/5 d)		1.04	3.6	3.4	940	0.33
14	22	1 (130/10/5 d)	3.83[k]					

[a] Chain length of the surfactant. [b] The solid product was filtered and resuspended in water between the treatments (reaction temperature/ value during the first treatment/complete treatment period in weeks (w) or days (d)). [c] $a = d_{hkl}(h^2 + k^2 + l^2)^{1/2}$ is a cubic lattice parameter calculated from PXRD (e.g., $a = 6^{1/2}d_{211}$), from calcined materials. [d] BJH desorption cumulative pore volume of pores between $d_P = 1.5$ and 6.5 nm; all samples were pretreated at 250 °C in vacuo until the pressure was $<10^{-3}$ Torr. [e] Pore diameter according to the maximum of the BJH pore size distribution calculated from the adsorption or desorption branch, respectively, (fwhm = full width at half-maximum). [f] Specific BET surface area. [g] Mesoporosity index M. [h] Specific surface area estimated from the pore volume and pore diameter assuming a M value of 0.35. [i] The first hydrothermal treatment was carried out with the original reaction mixture. [j] Presence of micropores. [k] Identification of a 100% lamellar phase after 3 d.

thermal treatments, a MCM-48 sample with pore diameters of 2.8 nm was obtained;[14] details of the use of a *long-chain* surfactant ($n = 21$) were not published.[15] Herein we present the synthesis of MCM-48 silicas with adjustable pore diameters via an advanced *gemini* surfactant approach. Moreover, we introduce the mesoporosity index M as a valuable tool to characterize porous materials and estimate the real pore size by correlating PXRD and N_2-physisorption data.

Experimental Section

Surfactants. The *gemini* surfactants $[CH_3(CH_2)_nNMe_2(CH_2)_mNMe_2(CH_2)_nCH_3]^{2+}2Br^-$ ($m = 12$, C_{n-12-n}) were synthesized employing slightly modified literature procedures.[17,18] Docosyldimethylamine was prepared by reacting metalorganic $LiNMe_2$ (Aldrich) with $C_{22}H_{45}Br$ (Aldrich) in dry ether in a molar ratio of 1.05:1. After being stirred for 20 min the solvent was removed in vacuo. Purification of the docosyldimethylamine was accomplished by recrystallizing the hydrochloride from hexane/ethanol and subsequent extraction with hexane; its purity was checked by gas chromatography. The alkylammonium salt $CH_3(CH_2)_{21}NMe_3Br$ (C_{22}) was synthesized and purified as described in ref 19. The *divalent* surfactant $[CH_3(CH_2)_{21}NMe_2(CH_2)_3NMe_3]^{2+}2Br^-$ (C_{22-3-1}) was synthesized from docosyldimethylamine and (3-bromopropyl)trimethylammonium bromide.

Syntheses. In a typical synthesis (material **10**), 46.4 g TEOS (Fluka) was added to a solution of 10.0 g surfactant $C_{22-12-22}$ and 37.0 g NMe_4OH (25 wt % solution in water, Aldrich) in 400 g of H_2O. After being stirred for a time period < 1 h, the solid product was recovered by filtration, resuspended in deionized water, and hydrothermally posttreated by variation of parameters T, t, and pH as described in Table 1. The pH value was adjusted by application of a buffer solution or addition of some mother liquor (pH = 12.5). While slight deviations from the molar ratios were tolerated by the product, a high purity of the surfactants was essential. Molar gel compositions (buffer system) were as follows: samples **1**−**5**, 1, TEOS, 0.47 NMe_4OH, 0.043, $C_{16-12-16}$, and 130, H_2O; sample **6**, 1, TEOS, 0.47, NMe_4OH, 0.026, $C_{16-12-16}$, 0.026, $C_{22-12-22}$, and 130, H_2O; samples **7**, **9**, and **12**, 1, TEOS, 0.47, NMe_4OH, 0.043, $C_{22-12-22}$, and 100, H_2O; sample **8**, 1, TEOS, 0.47, NMe_4OH, 0.043, $C_{22-12-22}$, and 110, H_2O (0.05 N $NaHCO_3$/0.2 N Na_2CO_3); samples **10** and **11**, 1, TEOS, 0.47, NMe_4OH, 0.043, $C_{22-12-22}$, and 100, H_2O (mother liquor); sample **13**, 1, TEOS, 0.47, NMe_4OH, 0.043, $C_{22-12-22}$, and 200 H_2O (0.8% KH_2PO_4); sample **14**, 1 TEOS, 0.47, NMe_4OH, 0.043, $C_{22-12-22}$, and 200 H_2O (mother liquor).

Analyses. X-ray powder diffraction patterns were recorded on a Huber instrument in the step/scan mode (samples **1**, **5**, **12**; step width, 0.016; accumulation time, 5 s/step; range (2θ), 1.0−9.0°) and on a Siemens D5000 instrument (sample **10**; step width, 0.005; accumulation time, 5 s/step; range (2θ), 1.0−9.0°) using monochromatic Cu Kα radiation ($\lambda = 0.154\,05$ nm). IR spectra were recorded on a Perkin-Elmer FTIR spectrometer, 1760X, using Nujol mulls between CsI plates. Nitrogen adsorption−desorption isotherms were measured with an ASAP 2010 volumetric adsorption apparatus (Micromeritics) at 77.4 K [$a_m(N_2, 77\ K) = 0.162$ nm^2]. The samples were outgassed in the degas port of the adsorption analyzer as indicated in Table 1. The BET specific surface area was obtained from the nitrogen adsorption data in the relative pressure range from 0.04 to 0.2.[20] The pore size distributions were derived from the desorption branches using the BJH method.[21] The surface silanol population was obtained from the surface coverage $\alpha(SiR_3)$ (carbon content, Elementar VarioEL/Perkin-Elmer) of activated silylated samples as described previously.[3c]

Results and Discussion

Purely siliceous MCM-48 with different pore diameters were hydrothermally synthesized and characterized by PXRD (powder X-ray diffraction), nitrogen physisorption, and surface silylation. By variation of the average chain length ($n + 1$) of the *gemini* $[CH_3(CH_2)_nNMe_2(CH_2)_mNMe_2(CH_2)_nCH_3]^{2+}2Br^-$ ($m = 12$, C_{n-12-n}) cationic alkylammonium surfactants and of the hydrothermal parameters (temperature T, pH, time period

(16) (a) Morey, M. S.; Davidson, A.; Stucky, G. D. *Microporous Mater.* **1996**, *6*, 99. (b) Morey, M. S.; O'Brien, S.; Schwarz, S.; Stucky, G. D. *Chem. Mater.* **2000**, *12*, 898.

(17) Goerderler, J. In *Houben-Weyl*; Müller, E., Ed.; Georg Thieme Verlag: Stuttgart, Germany, 1958; Volume 11/2, p 591.

(18) Zana, R.; Bennraou, M.; Rueff, R. *Langmuir* **1991**, *7*, 1072.

(19) Bacaloglu, R.; Bunton, C. A.; Ortega, F. *J. Phys. Chem.* **1989**, *93*, 1497.

(20) Sing, K. S. W.; Everett, D. H.; Haul, H. R. A. W.; Moscou, L.; Pierotti, R. A.; Rouquérol, J.; Siemieniewska, T. *Pure Appl. Chem.* **1985**, *57*, 603.

(21) Barret, E. P.; Joyner, L. G.; Halenda, P. P. *J. Am. Chem. Soc.* **1951**, *73*, 373.

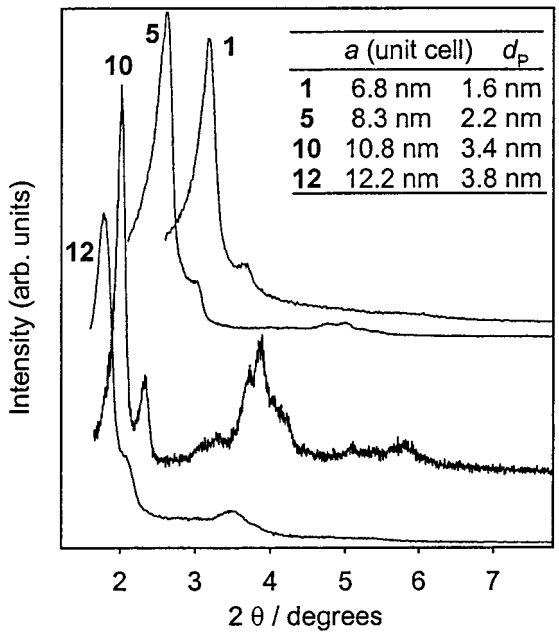

Figure 1. X-ray powder diffractogramms of calcined MCM-48 materials **1**, **5**, **10** and **12** (813 K/6 h).

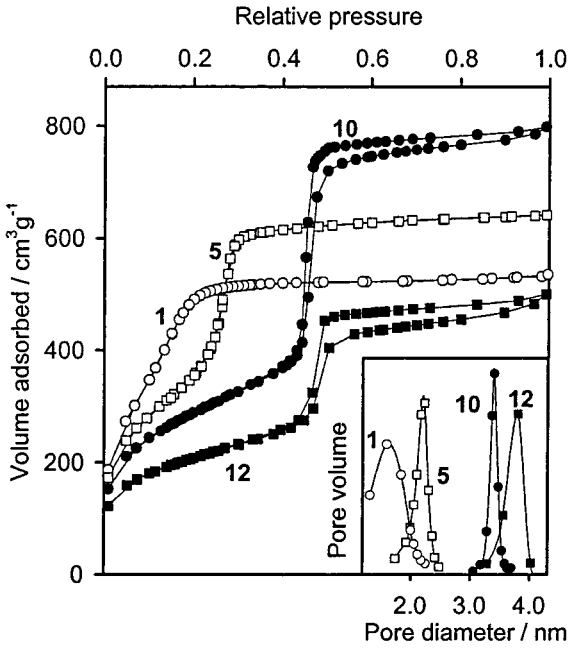

Figure 2. N_2 physisorption isotherms and pore size distributions of MCM-48 materials **1**, **5**, **10** and **12** (cf. Table 1).

t), cubic PMSs samples **1**−**13** were obtained with BJH pore diameters ranging from 1.6 to 3.8 nm. The PXRD pattern of the calcined samples were characteristic of well-ordered materials and are representatively shown for materials **1**, **5**, **10**, and **12** in Figure 1 (for cubic lattice parameter *a*, see Table 1).

The nitrogen adsorption−desorption isotherms of the calcined samples **1**, **5**, **10**, and **12** are shown in Figure 2. They exhibit sharp capillary condensation steps centered at relative pressures between 0.20 and 0.50, indicating a wide range of average pore sizes (values of V_p and d_p are listed in Table 1). Although the BJH method is generally applied to determine the pore size distribution of PMSs, alternative adsorption methods[22] as well as theoretical and geometrical calculations

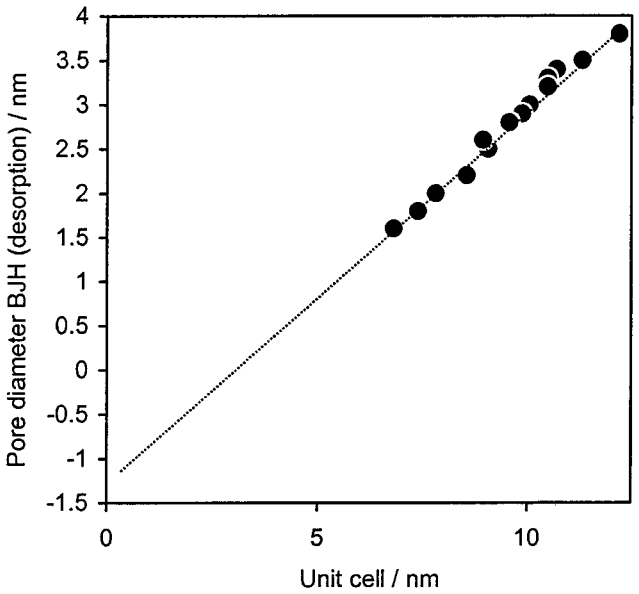

Figure 3. Correlation of the unit cell size with the BJH pore diameter.

showed that the effective pore diameter is underestimated.[23,24] Nevertheless, we and other groups found that *relative* changes of the pore size can be reliably investigated by the BJH method.[25−27] To reveal the real pore size we correlated the BJH pore diameter (derived from the desorption branch of the isotherm) with the corresponding size of the unit cell (Figure 3). The linear correlation of these data confirms that relative changes of the pore size are sufficiently accounted for and that the effective BJH pore diameter is underestimated by ca. 1.2 nm as derived from the intersection of the extended linear curve and the *y*-axis. This is in accordance with theoretical investigations presented recently.[23]

Furthermore, to analyze porosity features, we would like to introduce the mesoporosity index *M* (eq 1). *M*

$$M = \frac{V_P}{a_{s,BET} d_p} \qquad (1)$$

represents a congruence relation defined by the maximum of the BJH pore size distribution (d_P, derived from the desorption branch), the specific BET-surface area (a_s), and the cumulative BJH pore volume (here: V_P for $1.5 < d_P < 6.5$ nm). Consequently, the theoretical value of a cylindrical pore amounts to $M = 0.25$. Although the porosity data obtained via the BJH and BET methods are full of inaccuracies, eq 1 seems to provide distinct values *M* for high quality MCM-48 (*M* 0.34−0.35) and

(22) (a) Galarneau, A.; Desplantier, D.; Dutartre, D.; Di Renzo, Francesco, *Microporous Mesoporous Mater.* **1999**, *27*, 297−308. (b) Lukens, W. W., Jr.; Schmidt-Winkel, P.; Zhao, D.; Feng, J.; Stucky, G. D. *Langmuir* **1999**, *15*, 5403.

(23) Kruk, M.; Jaroniec, M.; Sayari, A. *Chem. Mater.* **1999**, *11*, 492.

(24) (a) Ravikovitch, P. I.; O'Domhnaill, S. C.; Neimark, V. A.; Schüth, F.; Unger, K. K. *Langmuir* **1995**, *11*, 4765. (b) Ravikovitch, P. I.; Wei, D.; Chueh, W. T.; Haller, G. L.; Neimark, V. A. *J. Phys. Chem., B* **1997**, *101*, 3671. (c) Ravikovitch, P. I.; Neimark, V. A. *Langmuir* **2000**, *16*, 2419.

(25) Luan, Z.; Maes, E. M.; van der Heide, P. A. W.; Zhao, D.; Czernuszewicz, R. S.; Kevan, L. *Chem. Mater.* **1999**, *11*, 3680.

(26) Widenmeyer, M.; Grasser, S.; Köhler, K.; Anwander, R. *Microporous Mesoporous Mater.* **2001**, *44*−*45*, 137.

(27) Nagl, I.; Widenmeyer, M.; Anwander, R. *Microporous Mesoporous Mater.* **2001**, *44*−*45*, 311.

MCM-41 materials (M 0.29−0.31).[28] More importantly, M seems to give a reliable indication of microporosity in meso and macroporous solids. For example, materials **11** and **12** display a considerable amount of micropores as indicated by their low values M of 0.31 and 0.26, respectively. The presence of micropores, which is also in accordance with the *t*-plot analysis, can be ascribed to the formation of some nonordered amorphous silica. Moreover, SBA-15 materials exhibit very low values M, and a closer look at the physisorption data reveals that a considerable amount of the specific surface area is attributed to smaller mesopores and/or micropores.[28,29] Also, MCF materials[30] exhibit a high degree of microporosity according to very low M values. The BET method often produces abnormally high surface areas for PMSs with pores < 2 nm, for example, 2400 $m^2\ g^{-1}$ for sample **2**. This is caused by the overlap of the BET area (monolayer formation) and the region of capillary condensation as evidenced for the isotherm of material **1** in Figure 2. We have applied eq 1 to estimate the surface area of MCM-48 samples **1**-**3** for a fixed value M of 0.34 and consider thus calculated values a_s (ca. 1500 $m^2\ g^{-1}$) as more realistic.

MCM-48 materials with pore diameters between 1.6 and 2.2 nm were obtained by using the $C_{16-12-16}$ surfactant ($n = 15$). The *longer-chain* structure-directing reagent $C_{22-12-22}$ ($n = 21$) afforded BJH pore diameters between 2.8 and 3.8 nm. Within this range, pore size control could be achieved by hydrothermal posttreatment procedures.[31] Materials **1**, **2**, **6**, and **7**, obtained at pH values <9 and at 100 °C, exhibit relatively broad pore size distributions (fwhm ≈ 0.5 nm), a marked shrinkage of the unit cell during calcination (e.g., Δd_{211}-(sample **1**) = 0.68 nm), and as a consequence smaller pore sizes. Interestingly, these materials show comperatively high specific surface areas and pore volumes. This can be attributed to the formation of smaller pore wall thicknesses during the hydrothermally induced reorganization and ordering processes of the silica framework. At lower pH values, Si−O−Si bond disruption and recondensation processes are kinetically disfavored. Sample **1** shows a remarkably small pore size of "1.6 nm", which is corroborated by the size of its unit cell being as low as 6.8 nm.

The formation of more stable pore walls is kinetically favored only at higher temperatures or higher pH values. The presence of thicker pore walls seems to be an important feature of materials with very narrow pore size distributions and enlarged pores. This can be accomplished by adjusting the pH values between 9 and 12.5 during the first hydrothermal treatment (samples **5** and **8**);[32] for further quality increase, subsequent treatments at a lower pH values (pH = 7−9) were advantageous. Additionally, the temperature T and the treatment period t affect the pore sizes. Figure 4 shows the enlargement of the unit cell parameter a dependent on the duration of the hydrothermal treatment during the synthesis of material **11**. Furthermore, $C_{22-12-22}$-based materials revealed pore diameters of 3.2 (**10**), 3.4 (**11**), and 3.8 nm (**12**) after treatment at 100, 110, and 130 °C, respectively. We suppose a restructuring process at such elevated temperature which is dominated by the packing of the electrostatically interacting ammonium headgroups at the organic−inorganic interface. Although material **12** showed a considerable decrease of surface area and pore volume, its structural collapse was not indicated by PXRD (Figure 1). Multiple hydrothermal posttreatment at 130 °C and pH 7 did not further enlarge the pore diameter (sample **13**). However, hydrothermal posttreatment at 130 °C and higher pH resulted in the formation of a lamellar phase as revealed by the PXRD pattern of as-synthesized sample **14**.[31a] In the literature, partly contrary explanations are given for pore size expansion during postsynthesis hydrothermal restructuring. For example, partial decomposition of the surfactant to yield the corresponding amine, which penetrates into the hydrophobic region of the micelle, thus increasing its size, was discussed for MCM-41 materials. The occurrence of amine was confirmed by ^{13}C CP MAS NMR spectroscopy.[5] However, in another study, no evidence of surfactant decomposition was found by ^1H NMR spectroscopy of solvent-extracted as-synthesized and aged PMS samples.[8a]

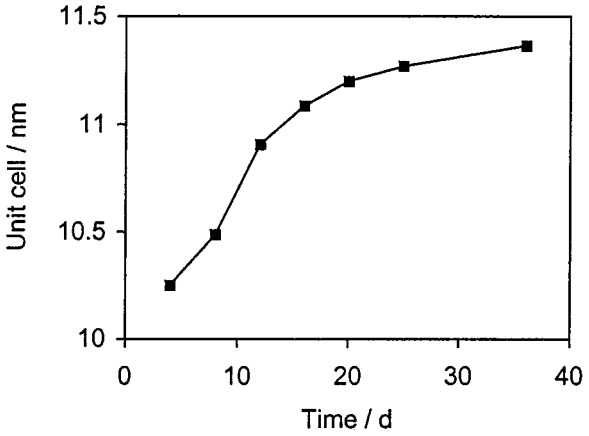

Figure 4. Change of the unit cell size during the hydrothermal synthesis of sample **11**.

The pore size gap between 2.2 and 2.8 nm could be filled by the use of a mixture of *gemini* surfactants. An equimolar mixture of $C_{22-12-22}$ and $C_{22-16-22}$ produced a well-ordered MCM-48 material **6** with a pore diameter of 2.5 nm (Table 1). Note that mixtures of *gemini* and *divalent* alkylammonium salts, for example, $C_{22-12-22}$ and C_{22-3-1} (2:1-ratio), and mixtures of *gemini* and *one-chain one-charge headgroup* surfactants, for example, $C_{22-12-22}$ and C_{22} (1:1-ratio), formed purely lamellar and mixed lamellar/MCM-48 silica phases.[28]

A silylation study was performed in order to examine the effect of the pore size on the surface morphology. After careful dehydration of the calcined materials, the

(28) Widenmeyer, M. Ph.D. Thesis, Technische Universität München, 2001.

(29) (a) Lukens, W. W.; Schmidt-Winkel, P.; Zhao, D.; Feng, J.; Stucky, G. D. *Langmuir* **1999**, *15*, 5403. (b) Kruk, M.; Jaroniec, M.; Ko, C. H.; Ryoo, R. *Chem. Mater.* **2000**, *12*, 1961. (c) Impéror-Clerc, M.; Davidson, P.; Davidson, A. *J. Am. Chem. Soc.* **2000**, *122*, 11925. (d) Miyazawa, K.; Inagaki, S. *Chem. Commun.* **2000**, 2121. (e) Göltner, C. G.; Smarsly, B.; Berton, B.; Antonietti, M. *Chem. Mater.* **2001**, *13*, 1617.

(30) (a) Schmidt-Winkel, P.; Lukens, W. W.; Zhao, D. Y.; Yang, P. D.; Chmelka, B. F.; Stucky, G. D. *J. Am. Chem. Soc.* **1999**, *121*, 254. (b) Schmidt-Winkel, P.; Luskens, W. W., Jr.; Yang, P.; Margolese, D. I.; Lettow, J. S.; Ying, J. Y.; Stucky, G. D. *Chem. Mater.* **2000**, *12*, 686. (c) Lukens, W. W.; Yang, P.; Stucky, G. D. *Chem. Mater.* **2001**, *13*, 28.

(31) (a) Corma, A.; Kan, Q.; Rey, F. *Chem. Commun.* **1998**, 579. (b) Chen, L.; Horiuchi, T.; Mori, T.; Maeda, K. *J. Phys. Chem., B* **1999**, *103*, 1216.

(32) Wang, A.; Kabe, T. *Chem. Commun.* **1999**, 2067.

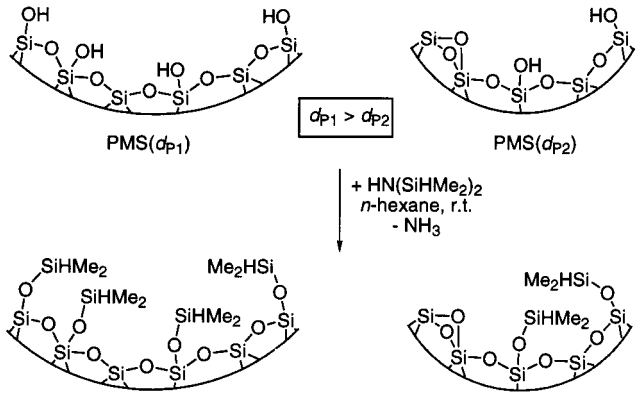

Figure 5. Schematic drawing of varying surface silanol densities at different pore sizes/surface curvatures.

number of surface hydroxyl groups of several samples was determined by silylation with tetramethyldisilazane, HN(SiHMe$_2$)$_2$.[3c] Note that high quality materials revealed complete consumption of the silanol groups as evidenced by FT IR spectroscopy. The surface density of SiOH groups seems to increase with the pore diameter, and hence with decreasing surface curvature (Figure 5). For example, materials **3** (2.1 nm), **6** (2.6 nm), and **11** (3.4 nm) exhibit 1.4, 1.75, and 1.9 SiOH groups per nm^2, respectively. The silanol group population has important implications not only for the surface polarity and hydrophobicity. It also directs the podality of grafted metal centers, i.e., the number of covalent M−O(support) bonds, and hence their activity in catalytic transformations.[27,29] The silylation experiments also revealed that a significant amount of SiOH groups of material **12** was not accessible to tetramethyldisilazane. This can be attributed to the presence of a significant amount of SiOH groups located in micropores, which is in accordance with the remarkably low *M* values of these materials.

Conclusions

Highly ordered cubic mesoporous silica MCM-48 with tunable pore sizes in the range 1.6−3.8 nm have been reproducibly synthesized via the *gemini* surfactant approach utilizing cationic $C_{22-12-22}$ and $C_{22-16-22}$ alkylammonium salts. Both surfactant average chain length and purity and hydrothermal treatment conditions comprising pH values >9 and temperatures >100 °C are important factors to govern the pore size and crystallinity. Mixtures of *gemini* surfactants facilitate the synthesis of materials featuring pores of medium size. The mesoporosity index *M* displays a simple means to examine the quality of PMS materials with respect to phase purity and porosity features (mesoporosity vs microporosity). Finally, tetramethyldisilazane, HN(SiHMe$_2$)$_2$, exhibiting a higher silylation efficiency in comparison to the commonly used standard silylation reagent hexamethyldisilazane, HN(SiMe$_3$)$_2$, proves to be an ideal reagent to examine the surface morphology of PMS materials. For example, the dehydrated MCM-48 samples under study revealed a different surface silanol population dependent on the pore size, that is, dependent on the curvature of the pore walls. Note that the number and distribution of surface silanol groups have important implications for the postsynthetic functionalization of PMS materials for catalytic applications.

Acknowledgment. We thank the Deutsche Forschungsgemeinschaft for financial support. Generous support from Prof. W. A. Herrmann is gratefully acknowledged.

CM011273B